

# Ionogel Fiber Mats: Functional Materials *via* Electrospinning of PMMA and the Ionic Liquid Bis(1-butyl-3-methyl-imidazolium) Tetrachloridocuprate(II), [Bmim]<sub>2</sub>[CuCl<sub>4</sub>]

Christian Bagdahn and Andreas Taubert

Institute of Chemistry, University of Potsdam, Karl-Liebknecht-Str. 24–25, D-14476 Potsdam, Germany

Reprint requests to A. Taubert. Tel. 0049 (0)331 977 5773. E-mail: [ataubert@uni-potsdam.de](mailto:ataubert@uni-potsdam.de).

Web: [www.taubert-lab.net](http://www.taubert-lab.net)

*Z. Naturforsch.* **2013**, *68b*, 1163–1171 / DOI: 10.5560/ZNB.2013-3195

Received July 19, 2013

Ionogel fiber mats were made by electrospinning poly(methylmethacrylate) (PMMA) and the ionic liquid (IL) bis(1-butyl-3-methyl-imidazolium) tetrachloridocuprate(II), [Bmim]<sub>2</sub>[CuCl<sub>4</sub>], from acetone. The morphology of the electrospun ionogels strongly depends on the spinning parameters. Dense and uniform fiber mats were only obtained at concentrations of 60 to 70 g L<sup>-1</sup> of polymer and IL mass combined. Lower concentrations led to a low number of poorly defined fibers. High voltages of 20 to 25 kV led to well-defined and uniform fibers; voltages between 15 and 20 kV again led to less uniform and less dense fibers. At 10 kV and lower, no spinning could be induced. Finally, PMMA fibers electrospun without IL show a less well-defined morphology combining fibers and oblong droplets indicating that the IL has a beneficial effect on the electrospinning process. The resulting materials are prototypes for new functional materials, for example in sterile filtration.

**Key words:** Ionic Liquid, Ionogel, Electrospinning, Fiber, Hydrogen Production, Filtration

## Introduction

Ionic liquids (ILs) are arguably among the most intensely researched areas in chemistry, physics and materials sciences. The reason for the ever increasing interest in ILs is the fact that they have technologically relevant properties such as low melting points, high solvation power, negligible vapor pressure, high ionic conductivity, broad electrochemical windows, and relatively good thermal stability [1–3]. A key advantage of ILs is the fact that – in principle – the synthesis of a large library of ILs with different and adjustable properties is straightforward; simply combining different anions and cations will yield ILs with different properties, although this is not always an easy task. Of particular interest to *functional* materials development are “inorganic” ILs, that is, ILs that contain one or more inorganic ions, because such ions will infer additional interesting properties such as magnetism, luminescence, optical, or catalytic activity to the respective ILs [4–12].

Tetrahalidometallate ILs, that is, ILs based on the  $MX_4^{n-}$  anion ( $M = e. g. Fe, Co, Ni, Cu, Zn, Au, Pd, Pb$ ;  $X = Cl^-, Br^-, I^-$ ;  $n = 1, 2$ ) have been reported by several research groups. Some of the work focused on catalysis [13–16]. The main focus has been on the formation and phase behaviour of the respective ILs and ionic liquid crystals (ILCs) [17–25]. Other work has focused on the synthesis of inorganic particles or on materials synthesis from the respective tetrahalidometallates or related pseudohalide-based ILs [26–32]. More recently Binnemans and coworkers have reported on what they call “liquid metal salts”, that is, ILs where the cation, not the anion, is based on a metal ion [33].

In one example of bringing metal-based ILs into the realm of applications, Gilmore *et al.* have shown that both the structure of the cation and the chemistry of the metal ion (silver vs. copper) affect the overall toxicity and antibacterial activity of Cu- and Ag-based imidazolium ILs [34]. As a tuneable toxicity in principle enables a tuneable antibiotic activity, this report sug-

gests that metal-containing ILs could be attractive for the fabrication of sterile or antiseptic materials. To that end, however, the ILs must be incorporated into a matrix such as wound dressings or filter materials.

An attractive method for incorporating ILs into a material is the fabrication of ionogels. Ionogels are IL/inorganic or IL/polymer hybrid materials combining the properties of the matrix such as mechanical robustness and the properties of the IL [35, 36]. Nowadays luminescent [37–39], photochemically active [40], magnetic [41, 42], proton- [43] and other ion-conductive [44, 45], along with mechanically robust ionogels with adjustable mechanical properties [46] are known. Most ionogels so far are bulk materials with low surface areas [35, 36]. For applications like sterile filtration, however, a mesh or fiber architecture with a fairly large surface and an adjustable porosity is necessary. One viable approach towards such high-surface area ionogels is electrospinning.

Electrospinning is a cheap and simple technology enabling the fabrication of large areas of fiber meshes of a defined fiber diameter, mesh size, film thickness, chemical composition, physical properties, and fiber orientation [47–50]. Electrospinning of ionogels is therefore a straightforward approach towards higher surface area materials of (functional) ionogels. The development of electrospun ionogels is, however, a relatively recent development, and the number of reports on the topic is still fairly limited.

Ertekin and coworkers developed mercury and iron sensors based on different dyes dissolved in an electrospun 1-ethyl-3-methyl-imidazolium tetrafluoroborate, [Emim][BF<sub>4</sub>]/ethyl cellulose nanofiber matrix [51–53]. The fibers show nanomolar sensitivity for Hg(II) and picomolar sensitivity for Fe(III) based on an optical readout. The same group also developed a CO<sub>2</sub> sensor using electrospun ionogels [54]. Shim and coworkers reported on vapor sensors for organic solvents (methanol, ethanol, 1-propanol, 1-butanol, tetrahydrofuran, acetone) based on electrospun poly(styrene/acrylonitrile)/1-butyl-3-methyl-imidazolium hexafluorophosphate, [Bmim][PF<sub>6</sub>], or nylon 6,6/[Bmim][PF<sub>6</sub>] nanofibers [55, 56]. Liu *et al.* obtained electrodes for the detection of dopamine, ascorbic acid, uric acid, guanine, and adenine from electrospun carbon nanofiber / 1-butyl-4-methyl-pyridinium hexafluorophosphate composite fibers [57].

Chinnappan *et al.* used ionogel nanofibers for the reduction of carbonyl compounds in aqueous NaBH<sub>4</sub>

solutions [58]. The same group also described catalytically active electrospun IL/polymer hybrid fibers for hydrogen production [59–61]. They used nickel and cobalt as catalytically active sites in the electrospun ionogel fibers for hydrogen release from sodium borohydride solutions. To our best knowledge, the two examples describing fibers modified with nickel-containing ILs [60, 61] are the first examples of electrospun fibers containing metal-based ILs.

A few other studies were also geared towards the general field of energy generation or storage. Pimenta *et al.* reported on the electrospinning of 1-(2-hydroxyethyl)-3-methyl-imidazolium tetrafluoroborate/gelatin fibers with high ionic conductivity [62]. Yee *et al.* used a post-electrospinning treatment with supercritical CO<sub>2</sub> to generate nanopores in poly(vinylidene fluoride) nanofiber membranes suitable for loading ILs [63]. The resulting materials have high ionic conductivities and could find application in electrochemical devices. Huang *et al.* prepared poly(vinylidene fluoride-co-hexafluoropropylene)/[Emim][BF<sub>4</sub>] nanofiber ionogels for use in double layer capacitors [64]. Cheruvally *et al.* reported on electrospun membranes of poly(vinylidene fluoride-co-hexafluoropropylene) with lithium bis(trifluoromethanesulfonyl)imide in 1-butyl-3-methyl-imidazolium bis(trifluoromethanesulfonyl)imide, [Bmim][N(Tf)<sub>2</sub>], or LiBF<sub>4</sub> in 1-butyl-3-methyl-imidazolium tetrafluoroborate, [Bmim][BF<sub>4</sub>] and their potential for use in lithium ion batteries [65].

Focusing on surface modification, Verma *et al.* fabricated non-wetting surfaces by electrospinning [Bmim][PF<sub>6</sub>]/poly(aryl ether) fibers [66]. The water contact angle (WCA) on the electrospun fiber mats increased from 90 to 150° on IL incorporation. In a similar approach, Lu *et al.* fabricated superhydrophobic surfaces from poly(styrene) (PS) and [Bmim][PF<sub>6</sub>] raising the WCA from 141 to 153°. Moreover, addition of the IL reduced the sliding angle from over 15° (pure PS fibers) to below 10° (ionogel fibers) [67].

Finally, a few studies have focused on the basics of the electrospinning process and the effects of electrospinning parameters on fiber formation when ILs are present. Yang *et al.* studied the electrospinning of polyacrylonitrile/1-butyl-3-methyl-imidazolium bromide solutions vs. spinning temperature and solution concentrations (*i. e.* viscosity) [68]. Heiden and coworkers investigated the role of additives, including ILs, on the electrospinning performance of poly(lactic

acid) and poly(vinyl alcohol) [69, 70]. All studies found a strong dependence on the solution concentrations and on the chemistry of the additive (IL or other).

Overall, the examples described above clearly show that electrospun ionogels may show significant application potential, but there is a need for more detailed information on the fabrication and properties of ionogel fiber mats. The current report therefore focuses on the fabrication of ionogel fiber meshes containing the IL bis(1-butyl-3-methyl-imidazolium) tetrachlorodocuprate(II), [Bmim]<sub>2</sub>[CuCl<sub>4</sub>]. In a proof-of-concept approach we show that it is possible to co-electrospin the IL with PMMA, leading to uniform fiber mats, so far with an IL loading of 10%. The fibers co-spun with the IL are more homogeneous than pure PMMA fibers spun under the same conditions. This is consistent with previous work [69, 70] and indicates that the IL also influences the spinning process as such. The results thus show that it is possible to fabricate ionogel fiber mats that could be attractive for, for example, sterile filtration by virtue of their high porosity and – at least by IL standards – relatively cheap antibacterial IL [34] contained within the fibers.

## Results

Mixtures of PMMA and [Bmim]<sub>2</sub>[CuCl<sub>4</sub>] in dry acetone are only homogeneous (one phase) up to a total content of PMMA and IL combined of 70 g L<sup>-1</sup>. Higher concentrations reproducibly lead to macroscopic phase separation making the electrospinning of solutions with solute concentrations above 70 g L<sup>-1</sup> into homogeneous materials difficult to impossible. We have therefore only used solutions with a total solute content of 70 g L<sup>-1</sup> or less for electrospinning. Moreover, it is not possible to obtain a jet at a high voltage (HV) lower than 15 kV. Between 15 and 25 kV, a jet forms, and the aluminum foil used as collector is covered with an off-white to light-yellow coating. The covered area is in all cases *ca.* 10 × 10 cm<sup>2</sup>.

Fig. 1 shows scanning electron microscopy (SEM) images of ionogel fibers. Although the fiber mats appear macroscopically homogeneous in all cases where a jet forms and a product can be collected on the collector, there are differences on the micrometer to nanometer level. Low concentrations of up to 40 g L<sup>-1</sup> (PMMA and IL combined) yield poor products; there are fibers but they coexist with droplets and islands not

connected to any of the fibers. Moreover, the fibers occasionally appear bimodal, that is, there are thin fibers with a diameter in the 100 to 200 nm range and thicker fibers with a diameter of around 500 nm. At very low concentrations of 20 g L<sup>-1</sup> and below, also numerous branch points between the fibers can be observed. In contrast, at concentrations between 60 and 70 g L<sup>-1</sup>, the fibers are uniform provided that the HV is 15 kV or higher. The most uniform fibers are obtained at concentrations of 70 g L<sup>-1</sup>.

Higher voltages favor a narrower size distribution, less bimodal diameter distributions, and fewer branch points, but this is, due to the significant sensitivity of the PMMA to the electron beam in the SEM, difficult to assess quantitatively. Overall, Fig. 1 shows that high concentrations of 60 or 70 g L<sup>-1</sup> and a HV of 20 or 25 kV are beneficial for the formation of uniform fiber mats.

Fig. 2 shows SEM images of PMMA electrospun under the same conditions but without addition of the IL. Fibers can be obtained but they exhibit a less uniform diameter than with the IL present in the spinning solution. Instead, the diameter varies, and the fibers have a pearl necklace-like morphology with oblong wider features and thinner sections. The diameter of the fibers in the thinner sections is comparable to the fibers shown in Fig. 1 (same conditions) at *ca.* 500 nm.

Fig. 3 shows representative attenuated total reflection infrared (ATR-IR) spectra of the precursors PMMA and [Bmim]<sub>2</sub>[CuCl<sub>4</sub>] along with a spectrum from an ionogel. The most obvious observation is that the IR spectra of the PMMA and the IL are less noisy than the spectra of the ionogels. We assign this to the fact that the amount of ionogel is relatively low and, correspondingly, the signals are also affected by the surrounding air atmosphere in the open area between the fibers.

IR spectra of pure [Bmim]<sub>2</sub>[CuCl<sub>4</sub>] show, in analogy to an earlier study by Hitchcock *et al.* [71], bands at 3140 and 3099 cm<sup>-1</sup> that are assigned to aromatic C–H stretching vibrations. Strong bands at 2959 and 2935 cm<sup>-1</sup> are assigned to aliphatic C–H stretching vibrations, while strong bands at 1568 and 1167 cm<sup>-1</sup> are due to imidazolium ring stretching vibrations. Less intense bands at 849 and 756 cm<sup>-1</sup> are from C–H in-plane bending vibrations, and bands at 652 and 623 cm<sup>-1</sup> are caused by asymmetric ring bending vibrations.

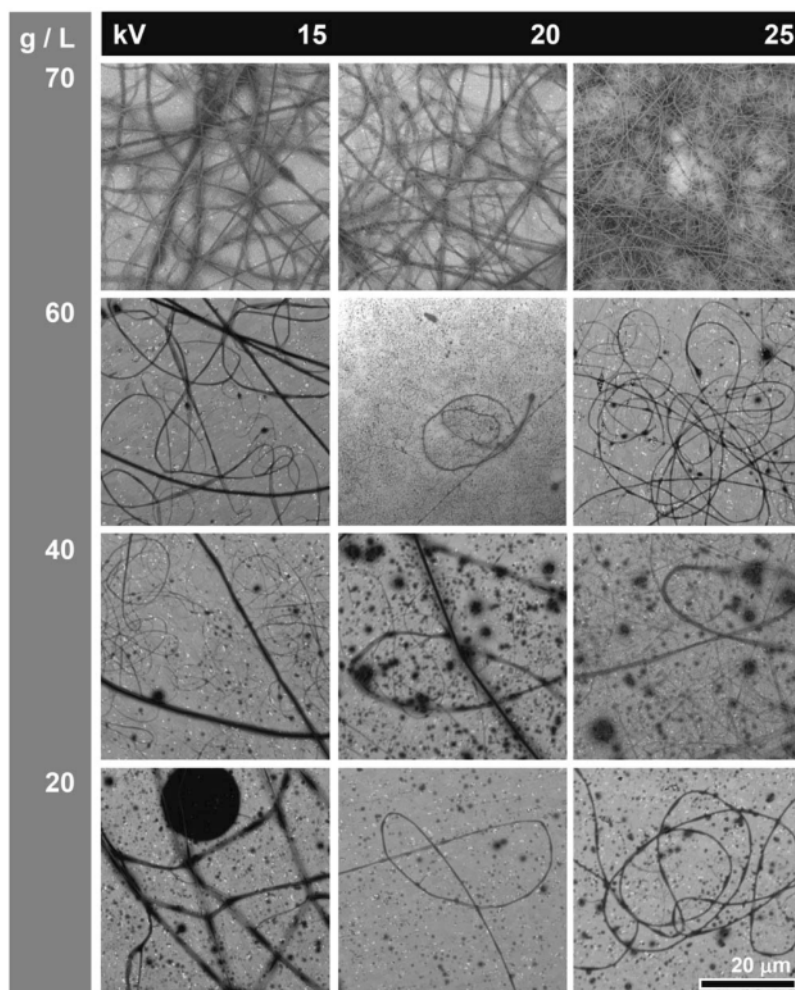


Fig. 1. SEM images of ionogels spun from dry acetone on aluminum foil vs. initial concentration and applied HV. Scale bar is identical for all images.

IR spectra of PMMA show intense bands at 1148 and 1191  $\text{cm}^{-1}$  from the C–O stretching vibration, at 1728  $\text{cm}^{-1}$  from the C=O stretching vibration, an intense band at 2950  $\text{cm}^{-1}$  from the symmetric C–H stretching vibration of the methyl ester, and a band at 2994  $\text{cm}^{-1}$  from the aliphatic C–H stretching vibration.

The spectra of the electrospun ionogels are a superposition of the two spectra of the individual components, similar to earlier work on PMMA/[Bmim][FeCl<sub>4</sub>] ionogels [39, 41]. The bands arising from the IL are weak or only present as shoulders in the ionogel spectra. However, a broad and weak band at 1569  $\text{cm}^{-1}$ , a shoulder at 1167  $\text{cm}^{-1}$ ,

and two very weak signals at 1336 and 1022  $\text{cm}^{-1}$  in the spectra of the ionogels indicate that the IL is incorporated into the ionogel. The low intensity of the IL signals is due to the fact that the ionogel fibers contain only 10% of IL (see Experimental Section for details); these low intensities correlate with earlier studies on ionogels with low IL fractions [41]. A further interesting observation is the absence of a water signal in the spectra of the ionogels in spite of the fact that both the IL and the PMMA exhibit broad bands at *ca.* 3500 and 3300  $\text{cm}^{-1}$ , respectively. This indicates that the electrospinning from dry acetone also removes most of the remaining water from the samples.

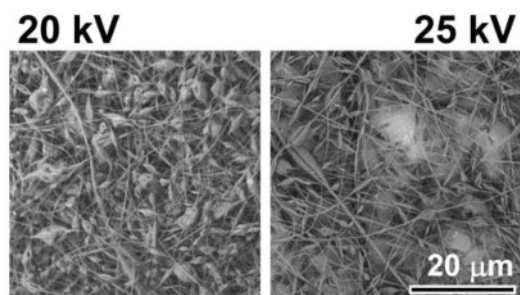


Fig. 2. SEM images of pure PMMA electrospun at 20 and 25 kV from solutions with  $70 \text{ g L}^{-1}$  solute concentration. Scale bar is identical for both images.

As stated in the introduction, copper-containing ILs have antimicrobial potential [34], and nickel-based electrospun ionogels have been successfully used in hydrogen production from  $\text{NaBH}_4$  solution [60, 61]. Ionogel fiber mats such as those presented here could therefore also be interesting for  $\text{NaBH}_4$  decomposition or sterile filtration. For example, exposure of the ionogel fiber mats to aqueous  $\text{NaBH}_4$  solutions could be used for controlled  $\text{NaBH}_4$  decomposition; possibly the rate of  $\text{NaBH}_4$  decomposition can be controlled by the fraction of IL in the ionogel fibers. The same concept could be used to adjust the antimicrobial performance of electrospun fiber mats by variation of the IL concentration or the chemical composition of the IL, especially the alkyl chain length of the imidazolium cation. Any of these applications, however, will inevitably have to deal with wetting issues. We have therefore evaluated the wetting behaviour of our ionogel fiber mats.

Fig. 4 shows representative images obtained from static water contact angle (WCA) measurements on an ionogel (10% IL) and PMMA (no IL) fibers prepared at the same spinning conditions (20 kV,  $60 \text{ g L}^{-1}$ ). The contact angles in both cases are high, but the addition of the IL leads to an increase of the WCA from  $128 \pm 0.05$  on pure PMMA to  $132 \pm 0.15$  on the ionogel.

## Discussion

Electrospinning is an attractive, yet cheap and simple technique for obtaining ionogel fiber mats. Optical inspection shows that in the present case, the miscibility of PMMA and  $[\text{Bmim}]_2[\text{CuCl}_4]$  with acetone may be a limiting step for the production of ionogel fibers

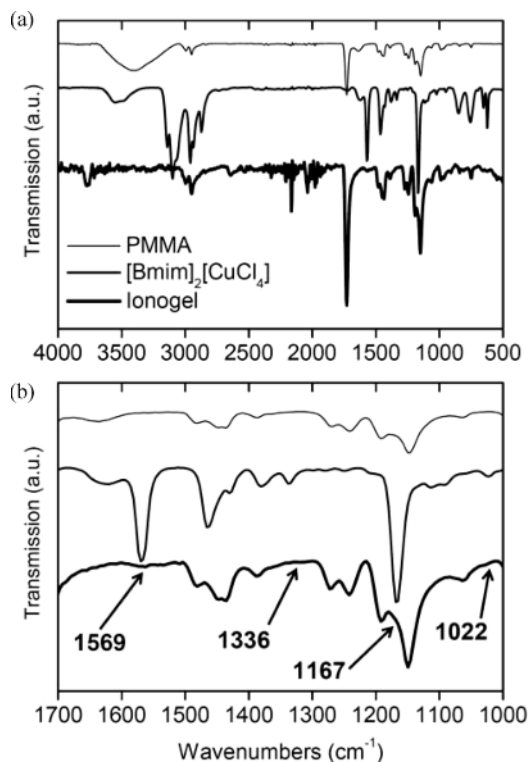


Fig. 3. ATR-IR spectra of neat PMMA, neat IL and ionogel electrospun at 20 kV and  $70 \text{ g L}^{-1}$ . (a) Full spectra, (b) magnified view of the region between 1700 and  $1000 \text{ cm}^{-1}$  to show the weak features mentioned in the text (highlighted by arrows). Bold numbers in panel (b) are the wavenumbers of band/shoulder positions in  $\text{cm}^{-1}$ .

with IL loadings much higher than 10%. SEM (Figs. 1 and 2) nevertheless shows that at concentrations between  $60$  and  $70 \text{ g L}^{-1}$  and at a HV of 20 or 25 kV (above the Rayleigh instability regime) [47], uniform fiber mats can be obtained. Consistent with literature [69, 70], the fibers are more homogeneous when the IL is present during electrospinning. IR spectra (Fig. 3) and, again consistent with literature [66, 67], increasing WCAs (Fig. 4) with IL incorporation, further show that also in the present case the IL is incorporated into the fibers. Co-electrospinning of PMMA and  $[\text{Bmim}]_2[\text{CuCl}_4]$  thus yields true ionogel fibers.

Ionogels are attractive materials for a number of applications, and quite some work has been devoted to the development of ionogels and the understanding of their formation, structure, properties, and property adjustment [35, 36]. In spite of the fairly large body of work that has been devoted to ionogels as

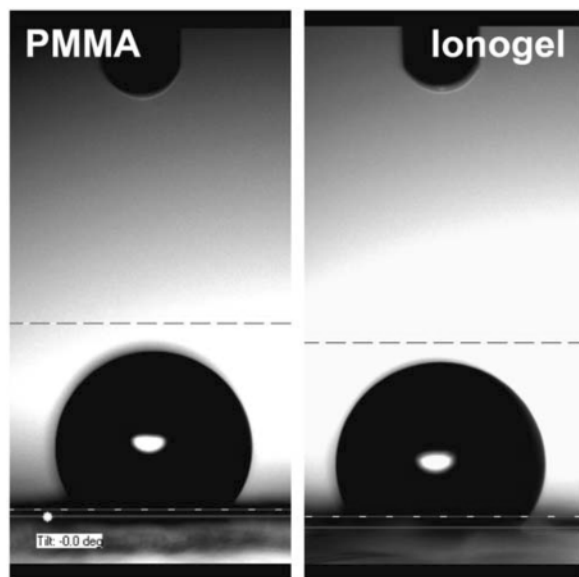


Fig. 4 (color online). Photograph of water droplets on electrospun PMMA fibers and ionogel fiber mats. Both samples were spun at 25 kV and from  $60 \text{ g L}^{-1}$  solutions.

such [35, 36], the vast majority of the reports is on bulk ionogels, that is, macroscopic objects or films. So far, still only just about 20 reports on electrospun ionogels have been published [51–58, 60, 62–70].

A significant fraction of the published work is devoted to sensors [51–57]. In principle, the ionogel fibers described here could also be used for sensing, for example when exploiting the ability of the Cu(II) ion to coordinate amines such as  $\text{NH}_3$ . Indeed, we do observe a reversible color change of the fiber mats from pale yellow to light green-blueish on exposure to ammonia vapor. However, attempts to read out the signal with a spectrometer or photometer have so far failed due to too weak signal intensities. This could possibly be improved by increased IL concentrations, but the solubility of  $[\text{Bmim}]_2[\text{CuCl}_4]$  in (dry) acetone is limited, and there are no simple alternative solvents that are able to dissolve both  $[\text{Bmim}]_2[\text{CuCl}_4]$  and PMMA in useful concentrations and still allow electrospinning. This thus limits the applicability of the current pair  $[\text{Bmim}]_2[\text{CuCl}_4]$  and PMMA to low IL loadings. In spite of these low IL loadings, the use of our ionogels as catalysts could be promising. Similar to existing systems [58, 60] our materials could be active in, for example,  $\text{NaBH}_4$  decomposition, similar to one of the examples by Kim and coworkers [60],

but further work will be necessary to evaluate this aspect.

Finally, consistent with reports by Lu *et al.* [67] and Verma *et al.* [66] we observe a higher static WCA on the ionogels than on the pure PMMA fibers. The effect is not as pronounced as in these articles, and the final WCA of  $132^\circ$  on the ionogel fibers is lower than those reported in the literature ( $150$  and  $153^\circ$ , respectively). However, in contrast to the hydrophobic IL  $[\text{Bmim}][\text{PF}_6]$  used in the two other studies, the IL used in this study,  $[\text{Bmim}]_2[\text{CuCl}_4]$ , is water-soluble and hydrophilic, and still the contact angle of the electrospun fiber meshes increases. This indicates that there are unresolved questions as to how ILs modify the surface of polymer fibers suggesting that the interaction of ILs and surfaces will need more attention in the future. This is further supported by findings from Heiden and coworkers on the effects of ILs on fiber morphology in electrospinning [69, 70]. The novelty of this material is thus the fact that it is the first example of copper-containing ionogels with a wide variety of potential applications.

## Conclusion

For reasons discussed throughout the text, ionogel fibers containing metal-based ILs such as  $[\text{Bmim}]_2[\text{CuCl}_4]$  are interesting from a basic scientific and engineering standpoint. The key issue of the current system is that the IL loading is, due to mutual solubility issues of PMMA and  $[\text{Bmim}]_2[\text{CuCl}_4]$ , relatively low at only a little over 10%. Further work will thus be necessary to identify more suitable polymer/IL combinations enabling higher IL loadings yielding materials that are interesting for applications such as those outlined above, for example catalysis, surface modification, and possibly sterile filtration.

## Experimental Section

### Materials

THF (Sigma-Aldrich,  $\geq 99\%$ ), ethanol (Merck, p. a.), chloroform (Sigma-Aldrich,  $\geq 99.8\%$ ), and copper(II) chloride dihydrate (Fluka,  $> 99\%$ ) were used as received. 1-Butyl-3-methyl-imidazolium chloride ( $[\text{Bmim}][\text{Cl}]$ , Aldrich, 95%) was recrystallized from the melt. To that end, the light-brown product was melted, and upon cooling colorless crystals formed above a dark-brown liquid phase. The colorless crystals were removed by filtration (G3 glass frit,

VWR) and washed with cold methyl-*t*-butyl ether (MTBE, Roth, > 99.5%). The purified compound was vacuum-dried and stored under Ar until further use. Methyl methacrylate (MMA, Alfa Aesar, 99%, *p*-methoxy phenol-stabilized) was filtered over basic alumina (Merck, 70–230 mesh, particle size 0.063–0.200 mm) to remove the inhibitor. Bis(azoisobutyronitrile) (AIBN, Fluka, > 98%, GC) was recrystallized from ethanol and chloroform. Acetone (VWR, > 99.8%) was dried over 3 Å molecular sieve (Fluka, molecular sieve UOP type 3A) and stored over 3 Å molecular sieve until further use.

### Synthesis

The synthesis of [Bmim]<sub>2</sub>[CuCl<sub>4</sub>] was adapted from similar systems [18–21, 27, 34, 72]. In a round bottom flask 17.47 g (0.1 mol) [Bmim][Cl] and 8.6 g (0.05 mol) CuCl<sub>2</sub>·2 H<sub>2</sub>O were mixed and stirred for 12 h at 60 °C. The resulting IL was dried for 24 h in high vacuum (0.003 mbar) to remove remaining water. Conversion was over 99%. Elemental Analysis: found (calculated): C 39.15 (40.36), H 6.26 (6.35), N 11.23 (11.73). – MS (ESI): *m/z* = 446, 448, 450 [M–Cl]<sup>+</sup>, 411, 413 [M–2Cl]<sup>+</sup>. – ATR-IR (neat substance, cm<sup>-1</sup>):  $\nu$  = 3140, 3099, 2959, 2935, 1568, 1167, 849, 756, 652, 623. – <sup>1</sup>H NMR (CD<sub>3</sub>OD, ppm vs. TMS):  $\delta$  = 0.55 (s), 1.01 (s), 1.54 (s), 3.60 (s), 3.86 (s), 4.24 (s), 7.18 (d, *J* = 11.2 Hz), 8.61 (s). Due to the broad signals in the NMR spectra of [Bmim]<sub>2</sub>[CuCl<sub>4</sub>], the assignments of the NMR signals was supported by comparison with the corresponding spectrum of [Bmim][Cl].

PMMA was synthesized *via* free radical polymerization. In a round bottom flask with Dimroth-cooler 12.22 g (0.112 mol) of MMA, 12.5 mL of THF and 0.13 g (0.8 mmol) of AIBN initiator were mixed, and the solution was stirred at 60 °C under Ar for 14 h. The PMMA was isolated by precipitation from an excess of water and subsequent drying. Further purification was achieved by repeated dissolution in acetone and precipitation from water. Yield after purification 10.84 g (89%). – <sup>1</sup>H NMR (CDCl<sub>3</sub>, ppm vs. TMS):  $\delta$  = 3.57 (s), 1.87 (s), 1.79 (s), 0.10 (s), 0.82 (s). – ATR-IR (neat substance, cm<sup>-1</sup>):  $\nu$  = 988, 1148, 1191, 1241, 1436, 1728, 2950, 2994. – GPC (THF, RI): *M<sub>n</sub>* = 125 kg mol<sup>-1</sup>, PDI = 2.05.

### Electrospinning

Ionogels were electrospun using a home-built setup with acceleration voltages up to 25 kV with horizontal spinning geometry. PMMA and [Bmim]<sub>2</sub>[CuCl<sub>4</sub>] were dissolved in dry acetone (wet acetone significantly deteriorates the quality of the obtained fibers). The weight ratio of PMMA to IL was always 9 : 1 (10% of IL), and the total concentration of dissolved matter (PMMA + IL) was varied from 20 to 1100 g L<sup>-1</sup> acetone. The ionogels were electrospun on aluminum foil. The needle diameter was 0.8 mm (Braun Sterican 0.8 × 120 mm), the needle-collector distance was 10 cm, the high voltage 5–25 kV, and the feeding rate 0.6 mL h<sup>-1</sup>.

### Instrumentation

Static contact angles were determined with a Cam100 contact angle meter (KSV Instruments Ltd., Espoo, Finland) using 3.56 μL (3.56 ± 0.26 mg) of de-ionized water (Millipore®, resistance 18.2 mΩ, TOC 2 mg L<sup>-1</sup>). SEM experiments were carried out on an FEI Phenom operated at 5 kV. Samples were mounted on aluminum SEM stubs *via* conductive carbon tape without removing the aluminum collector foil. Samples were imaged without sputtering or carbon coating. Mass spectrometry was performed on an ESI-Q-TOF maXis (UHR-TOF MS, Bruker Daltonik GmbH). GPC measurements were made with a Thermo Separation Products (TSP) GPC (detector: Shorex RI-71; standard: PMMA, solvent: THF; column PSS/SDV-VS+10E3+10E5+10E6). ATR-IR spectra were obtained on a NEXUS FT-IR spectrometer (Thermo-Nicolet, Diamond, ATR correction was done *via* Omnic 8.1.11; Thermo Fischer Scientific Inc.), and <sup>1</sup>H NMR measurements were carried out with Bruker Avance 300 (300 MHz) and Avance 500 (500 MHz) spectrometers. Elemental Analysis was made with a Vario EL III elemental analyzer.

### Acknowledgement

We thank A. Krtitschka, Dr. M. Heydenreich and Dr. I. Starke for help with NMR and ESI-TOF-MS measurements, Y. Linde for elemental analysis, and M. Gräwert for GPC measurements. The University of Potsdam is acknowledged for financial support.

- 
- [1] P. Wasserscheid, T. Welton (Eds.), *Ionic Liquids in Synthesis*, 2<sup>nd</sup> ed., Wiley-VCH, Weinheim 2007.
- [2] F. Endres, D. R. MacFarlane, A. Abbott (Eds.), *Electrodeposition from Ionic Liquids*, Wiley-VCH, Weinheim 2008.
- [3] B. Kirchner (Ed.), *Ionic Liquids*, Vol. 290, 1<sup>st</sup> ed., Springer, Heidelberg 2009.
- [4] J. Dupont, R. F. de Souza, P. A. Z. Suarez, *Chem. Rev.* 2002, 102, 3667.
- [5] T. Welton, *Coord. Chem. Rev.* 2004, 248, 2459.
- [6] I. J. B. Lin, C. S. Vasam, *J. Organomet. Chem.* 2005, 690, 3498.
- [7] K. Binnemans, *Chem. Rev.* 2005, 105, 4148.
- [8] K. Binnemans, *Chem. Rev.* 2007, 107, 2592.

- [9] K. Bica, P. Gaertner, *Eur. J. Org. Chem.* **2008**, 3235.
- [10] H. Olivier-Bourbigou, L. Magna, D. Morvan, *Appl. Catal. A* **2010**, 373, 1.
- [11] M. Petkovic, K. R. Seddon, L. P. N. Rebelo, C. S. Pereira, *Chem. Soc. Rev.* **2011**, 40, 1383.
- [12] L. Douce, J.-M. Suisse, D. Guillon, A. Taubert, *Liq. Cryst.* **2011**, 38, 1653.
- [13] K. Bica, P. Gaertner, *Org. Lett.* **2006**, 8, 733.
- [14] K. Bica, P. Gaertner, *Eur. J. Org. Chem.* **2008**, 3453.
- [15] M. Vasiloiu, P. Gaertner, K. Bica, *Sci. China: Chem.* **2012**, 55, 1614.
- [16] K. Bica, S. Leder, P. Gaertner, *Curr. Org. Synth.* **2011**, 8, 824.
- [17] C. J. Bowlas, D. W. Bruce, K. R. Seddon, *Chem. Commun.* **1996**, 1625.
- [18] F. Neve, A. Crispini, S. Armentano, *Chem. Mater.* **1998**, 10, 1904.
- [19] F. Neve, O. Francescangeli, A. Crispini, *Inorg. Chim. Acta* **2002**, 338, 51.
- [20] F. Neve, O. Francescangeli, A. Crispini, J. Charmant, *Chem. Mater.* **2001**, 13, 2032.
- [21] F. Neve, M. Imperor-Clerc, *Liq. Cryst.* **2004**, 31, 907.
- [22] R. Farra, K. Thiel, A. Winter, T. Klamroth, A. Pöpl, A. Kelling, U. Schilde, A. Taubert, P. Strauch, *New J. Chem.* **2011**, 35, 2793.
- [23] K. Thiel, P. Strauch, T. Klamroth, A. Taubert, *Phys. Chem. Chem. Phys.* **2011**, 13, 13537.
- [24] Z. L. Xie, A. Taubert, *ChemPhysChem* **2011**, 12, 364.
- [25] F. Neve, A. Crispini, *CrystEngComm* **2007**, 9, 698.
- [26] Z. Li, A. Friedrich, A. Taubert, *J. Mater. Chem.* **2008**, 24, 1008.
- [27] A. Taubert, *Angew. Chem. Int. Ed.* **2004**, 43, 5380.
- [28] A. Taubert, I. Arbell, A. Mecke, P. Graf, *Gold Bulletin* **2006**, 39, 205.
- [29] A. Taubert, C. Palivan, O. Casse, F. Gozzo, B. Schmitt, *J. Phys. Chem. C* **2007**, 111, 4077.
- [30] A. Taubert, P. Steiner, A. Manton, *J. Phys. Chem. B* **2005**, 109, 15542.
- [31] W. Dobbs, J. M. Suisse, L. Douce, R. Welter, *Angew. Chem. Int. Ed.* **2006**, 45, 4179.
- [32] R. Göbel, Z.-L. Xie, M. Neumann, C. Günter, R. Löb- bicke, S. Kubo, M.-M. Titirici, C. Giordano, A. Taubert, *CrystEngComm* **2012**, 14, 4946.
- [33] N. R. Brooks, S. Schaltin, K. Van Hecke, L. Van Meervelt, K. Binnemans, J. Fransaer, *Chem. Eur. J.* **2011**, 17, 5054.
- [34] B. F. Gilmore, G. P. Andrews, G. Borberly, M. J. Earle, M. A. Gilea, S. P. Gorman, A. F. Lowry, M. McLaugh- lin, K. R. Seddon, *New J. Chem.* **2013**, 37, 873.
- [35] J. Le Bideau, L. Viau, A. Vioux, *Chem. Rev.* **2011**, 40, 907.
- [36] A. Vioux, L. Viau, S. Volland, J. Le Bideau, *Compt. Rend. Chim.* **2010**, 13, 242.
- [37] K. Lunstroot, K. Driesen, P. Nockemann, C. Goerller- Walrand, K. Binnemans, S. Bellayer, J. Le Bideau, A. Vioux, *Chem. Mater.* **2006**, 18, 5711.
- [38] M. Czakler, M. Litschauer, K. Föttinger, H. Peterlik, M. A. Neouze, *J. Phys. Chem. C* **2010**, 114, 21342.
- [39] Z. L. Xie, H. B. Xu, A. Geßner, M. U. Kumke, M. Prie- be, K. M. Fromm, A. Taubert, *J. Mater. Chem.* **2012**, 22, 8110.
- [40] F. Benito-Lopez, R. Byrne, A. M. Raduta, N. E. Vrana, G. McGuinness, D. Diamond, *Lab Chip* **2010**, 10, 195.
- [41] Z. L. Xie, F. Wang, A. Jelicic, A. Friedrich, P. Rabu, S. Beuermann, A. Taubert, *J. Mater. Chem.* **2010**, 20, 9543.
- [42] B. Ziółkowski, K. Bleek, B. Twamley, K. J. Fraser, R. Byrne, D. Diamond, A. Taubert, *Eur. J. Inorg. Chem.* **2012**, 5245.
- [43] E. Delahaye, R. Göbel, R. Löb- bicke, R. Guillot, C. Sieber, A. Taubert, *J. Mater. Chem.* **2012**, 22, 17140.
- [44] T. Echelmeyer, H. W. Meyer, L. van Wüllen, *Chem. Mater.* **2009**, 21, 2280.
- [45] M. Henmi, K. Nakatsuji, T. Ichikawa, H. Tomioka, T. Sakamoto, M. Yoshio, T. Kato, *Adv. Mater.* **2012**, 24, 2238.
- [46] A. F. Visentin, M. J. Panzer, *ACS Appl. Mater. Inter- faces* **2012**, 4, 2836.
- [47] A. Greiner, J. H. Wendorff, *Angew. Chem. Int. Ed.* **2007**, 46, 5670.
- [48] I. Sas, R. E. Gorga, J. A. Joines, K. A. Thoney, *J. Polym. Sci. B: Polym. Phys.* **2012**, 50, 824.
- [49] S. Agarwal, A. Greiner, J. H. Wendorff, *Prog. Polym. Sci.* **2013**, 38, 963.
- [50] L. Persano, A. Camposeo, C. Tekmen, D. Pisignano, *Macromol. Mater. Eng.* **2013**, 298, 504.
- [51] S. Kacmaz, K. Ertekin, A. Suslu, Y. Ergun, E. Celik, U. Cocen, *Mater. Chem. Phys.* **2012**, 133, 547.
- [52] M. Z. Ongun, K. Ertekin, C. G. Hizliates, O. Oter, Y. Ergun, E. Celik, *Sens. Actuators, B* **2013**, 181, 244.
- [53] S. Kacmaz, K. Ertekin, M. Gocmenturk, A. Suslu, Y. Ergun, E. Celik, *React. Funct. Polym.* **2013**, 73, 674.
- [54] S. Aydogdu, K. Ertekin, A. Suslu, M. Ozdemir, E. Ce- lik, U. Cocen, *J. Fluoresc.* **2011**, 21, 607.
- [55] E. Kang, M. Kim, J. S. Oh, D. W. Park, S. E. Shim, *Macromol. Res.* **2012**, 20, 372.
- [56] M. Kim, E. Kang, D. W. Park, B. S. Shim, S. E. Shim, *Bull. Kor. Chem. Soc.* **2012**, 33, 2867.
- [57] Y. Liu, D. W. Wang, J. S. Huang, H. Q. Hou, T. Y. You, *Electrochem. Commun.* **2010**, 12, 1108.
- [58] A. Chinnappan, H. Kim, I. T. Hwang, *Chem. Eng. J.* **2012**, 191, 451.
- [59] A. Chinnappan, H. C. Kang, H. Kim, *Energy* **2011**, 36, 755.



- [60] A. Chinnappan, H. Kim, *Int. J. Hydrogen Energy* **2012**, *37*, 18851.
- [61] A. Chinnappan, H. Kim, C. Baskar, I. T. Hwang, *Int. J. Hydrogen Energy* **2012**, *37*, 10240.
- [62] A. F. R. Pimenta, A. C. Baptista, T. Carvalho, P. Brogueira, N. M. T. Lourenco, C. A. M. Afonso, S. Barreiros, P. Vidinha, J. P. Borges, *Mater. Lett.* **2012**, *83*, 161.
- [63] W. A. Yee, S. X. Xiong, G. Q. Ding, C. A. Nguyen, P. S. Lee, J. Ma, M. Kotaki, Y. Liu, X. H. Lu, *Macromol. Rapid Commun.* **2010**, *31*, 1779.
- [64] Z. B. Huang, D. S. Gao, Z. H. Li, G. T. Lei, J. Zhou, *Acta Chim. Sin.* **2007**, *65*, 1007.
- [65] G. Cheruvally, J. K. Kim, J. W. Choi, J. H. Ahn, Y. J. Shin, J. Manuel, P. Raghavan, K. W. Kim, H. J. Ahn, D. S. Choi, C. E. Song, *J. Power Sources* **2007**, *172*, 863.
- [66] R. Verma, N. Tomar, S. E. Creager, D. W. Smith, *Polymer* **2012**, *53*, 2211.
- [67] X. B. Lu, J. H. Zhou, Y. H. Zhao, Y. Qiu, J. H. Li, *Chem. Mat.* **2008**, *20*, 3420.
- [68] T. Yang, Y. Y. Yao, Y. Lin, B. Wang, R. L. Xiang, Y. R. Wu, D. C. Wu, *Appl. Phys. A: Mater. Sci. Process.* **2010**, *98*, 517.
- [69] J. M. Seo, G. K. Arumugam, S. Khan, P. A. Heiden, *Macromol. Mater. Eng.* **2009**, *294*, 35.
- [70] G. K. Arumugam, S. Khan, P. A. Heiden, *Macromol. Mater. Eng.* **2009**, *294*, 45.
- [71] P. B. Hitchcock, K. R. Seddon, T. Welton, *J. Chem. Soc., Dalton Trans.* **1993**, 2639.
- [72] F. Neve, O. Francescangeli, *Cryst. Growth Des.* **2005**, *5*, 163.